On a Model for Bone Remodeling: A Numerical and Analytical Assessment and Alternate Damage Dynamics

J. M. Restrepo
Department of Mathematics and Department of Physics
University of Arizona
Tucson, AZ 85721, U.S.A.

R. Choksi
Department of Mathematics
Simon Fraser University
Burnaby, BC V5A 1S6, Canada

Y. Jiang
Theoretical Division, Los Alamos National Laboratory
Los Alamos, NM 87545, U.S.A.

July 22, 2007

Abstract

We consider a phenomenological model for bone remodeling, proposed by Hazelwood *et al.* [1], which represents the process through a coupled population equation for basic multicellular units (BMUs) and a rate equation for microdamage. Its fundamental dependence on empirical data can lead to unbalanced model terms making any numerical approximations sensitive to implementation error. Thus we propose a balanced and simplified but equivalent restatement of the model. We show that, in this simpler guise, the model relates to more complex biologically-based models for bone remodeling, thus motivating a thorough analysis of its predictions as well as its robustness to modifications. We present a global analysis of the asymptotic solutions and study the model predictions numerically, with a computational algorithm that is shown to be stable. We also identify aspects of the model that could be parameterized with simpler alternatives.

We show that, if the rate of damage accumulation is independent of the damage itself (as in the original model), the damage will remain bounded in time even when severely over-stressed. To model bone failure under severe over-stress, we consider an alternative damage accumulation following a Paris law-like micro-crack dynamics. We show that such power-law damage accumulation does not alter substantially the outcomes of the under-stressed case; however, it allows for the possibility of irretrievable failure when the damage repair cannot counteract the growth term.

keywords: bone, remodeling, damage, BMU.

1 Introduction

Bone is a dynamic tissue that adapts its internal microstructure to its physiological and mechanical environment, through a process known as bone remodeling. Bone is continuously renewed and microdamage, accumulated by fatigue or creep, is continuously repaired. It is commonly accepted that bone remodeling is carried out by the basic multicellular units (BMUs), which consist of bone resorbing osteoclasts and bone forming osteoblasts working in concert. After the BMUs are activated, the following sequence of events occur: resorption of bone tissue for a time interval (the resorption period), a reversal time (the reversal period), the formation of new bone tissue.

A number of mathematical and computational models for bone remodeling have been proposed. Most of the earlier models are phenomenological descriptions of the average change of bone porosity or density by the coordinated activities of osteoclasts and osteoblasts. The recent advances in biologically-based models [1, 2, 3, 4, 5] have revealed a new phase of modeling for bone remodeling, which considers both bone cell activities and the mechanical effects. In particular, the coupling between fatigue damage dynamics (accumulation and removal) and the cell activities during bone remodeling as a function of mechanical stimulus has yielded fruitful results. We will refer to this class of models as a BMU-MD model. We focus here on a BMU-MD model proposed by Hazelwood, Martin, Rashid and Rodrigo [1] (referred to as HMRR), where the effects of the coupling between BMU dynamics and microdamage was first investigated. This model has been used to study the long-term effects of biphosphonate on the development of trabecular bone [6]. It has also been used in combination with a finite element code to assess different types of knee replacement strategies [7].

In Section 2 we restate the model proposed by HMRR. Doing so reveals its essential simple and robust structure and enables us to produce a mathematical characterization of its behavior; Section 3 presents an analysis of the equations. We show that the model can be solved algebraically, yielding the asymptotic outcomes in the long time limit. These steady states provide a global picture of the model outcomes and constrain the equilibrium values of bone porosity p and microdamage D. From the point of view of numerical analysis, the model entails a rather extreme range of parameters, making it extremely vulnerable to round-off error. In the Appendix we employ a stable numerical algorithm, and compare our results with those of Hazelwood *et al.* [1].

Our analysis suggests an important way in which the HMRR model can be refined. The HMRR model used a constant rate of accumulation of damage, which results in an upper bound for bone damage. Experimental data [8, 9, 10], however, show that repeated large loading continually weakens bone, and if the load is large enough the bone will eventually fail, *i.e.* damage becomes unbounded. We modify the damage accumulation equation to include an accumulation rate reminiscent of the Paris Law from fracture mechanics (cf. [11]). In Section 4 we show theoretically how this modification changes the outcomes when the bone is over-stresssed. Section 5 summarizes our results regarding the model analysis and how it is modified by using an alternative damage equation. In the Appendix we also consider ways in which the model can be simplified.

2 The BMU-MD Model

The aim of reformulating the model is to cast it in a simpler form, amenable to analysis. Unless otherwise noted, all choices of parameters, constitutive relations, and empirical functions, are taken directly from HMRR [1].

2.1 The physical variables

The model focuses on a representative volume of bone that contains BMUs. The external mechanical load on the representative volume affect the remodeling activities of BMUs, resulting in changes in bone porosity,

which in turn changes the mechanical response of the bone. This model reduces to a coupled system of integro-differential equations for the porosity $p(t)$ and the damage $D(t)$. Time t is measured in days. Porosity, given either as a fraction or as a percentage, represents the fraction of pores within the bone; $p = 0$ corresponds to dense bone, and $p = 1$ corresponds to bone of zero density. The damage is defined as the total crack length per section of area of the bone. The damage is non-negative for all time t. Two intermediate fields contribute to changes in p and D: a mechamical stimulus Φ, and the *activation frequency* $f_a(p, D, t)$.

The time to fracture resulting from a strain $\epsilon = L/(k_2 E)$ is given by the relation $t_f \propto \epsilon^{-q}$, where $q > 0$ is an empirically-adjusted exponent [9, 8], E is the elastic modulus of the bone, and ϵ is the strain. The mechanical stimulus is defined as

$$\Phi := \frac{1}{t_f} = R_L \, \epsilon^q, \tag{1}$$

where the constant R_L is the loading rate ([12]).

For the elastic modulus E, HMRR suggest the following polynomial fit to data, entirely in terms of the porosity p:

$$E(p) = 10^5 \left(8.83p^6 - 29.9p^5 + 39.9p^4 - 26.4p^3 + 9.08p^2 - 1.68p + 0.237\right). \tag{2}$$

Figure 1a shows E as a function of P. A composite of the elastic modulus appears in [13] and we note that the plotted polynomial fits well with the data for low porosity but differs greatly from the data at high porosity values. Figure 1c shows how a lower degree polynomial approximation compares to this high degree interpolant expression in (2), and how the modulus could be modified to decrease to zero in the high porosity regime. (Detailed discussion is in Appendix.)

We denote the empirically-derived *normalized specific surface area* as $S(p)$. A fit from data leads to

$$S(p) = \frac{1}{S_N} \left(28.8p^5 - 101.0p^4 + 134.0p^3 - 93.9p^2 + 32.2p\right), \tag{3}$$

where S_N normalizes the specific surface area to 1 and thus $S(p)$ is non-dimensional (see [14]). In Figure 1b we provide a plot of $S(p)$.

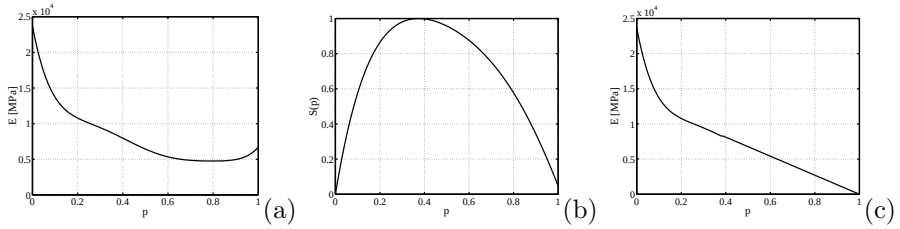

Figure 1: (a) Elastic modulus $E(p)$, (b) normalized specific area $S(p)$, and (c) hyperthetical elastic modulus, as a function of p. See [13] for details on the fit to data.

The BMU *activation frequency* $f_a(D, p)$ is given by

$$f_a(D, p) = S(p) \, (f_{a(disuse)}(p) + f_{a(damage)}(D)). \tag{4}$$

The part associated with disuse is defined as

$$f_{a(disuse)}(p) = \begin{cases} \frac{f_{a(max)}}{1 + c_1 \, e^{c_2 \Phi(p)}} & \text{if } \Phi < \Phi_0; \\ 0 & \text{otherwise,} \end{cases} \tag{5}$$

where Φ_0 is an empirical value estimated from cyclic strain levels needed to maintain cortical bone mass at equilibrium. The damage component is

$$f_{a(damage)}(D) = \frac{f_{a(max)}}{1 + c_3 \, e^{c_4 D}},$$

where $c_4 < 0$. The c_i are numerical constants, the values of which (and the connection with the constants in [1]) may be inferred from Table 1. (The Appendix includes an analysis of f_a and how it can be simplified.)

2.2 The coupled delay equations

For time $t \geq 0$, the BMU-MD equations for the porosity p and the damage D are

$$\frac{dp}{dt} = A\left(\overline{N_R}(p,D,t) - \overline{N_F}(p,D,t)\right) \tag{6}$$

$$\frac{dD}{dt} = K_D\Phi - F_s A\, D\, f_a(p,D), \tag{7}$$

Where K_D is a constant of proportionality (to be discussed further in Section 2.4), and $F_s = 5$ mm^{-2} is an empirical factor associated with microcrack surface area (see HMRR paper for details). There are three time intervals associated with the BMU activity: The resorption period T_R, the inactive period T_I, and the refilling period T_F. In the above equation, we have incorporated the temporal periods for both resorption and refilling via the averages $\overline{N_R}, \overline{N_F}$ (see (10) and (11)).The factor,

$$A = \begin{cases} A_0 & \text{if } \Phi \geq \Phi_0; \\ \frac{1}{2}A_0(1+\Phi/\Phi_0) & \text{otherwise,} \end{cases}$$

where A_0 is a given constant. It appears in every term on the right hand side of (6)-(7). The associated population resorption and refilling densities N_R and N_F at time t are given by

$$N_R = \int_{t-T_R}^{t} f_a(s)\, ds \qquad N_F = \int_{t-(T_R+T_I+T_F)}^{t-(T_R+T_I)} f_a(s)\, ds.$$

One must interpret the integrals for small times when their lower limits are negative. That is, as with any system of delay equations, one must prescribe initial data for $p(t)$ and $D(t)$ on the first full cycle of the BMU unit, i.e. for $t \in [0, T_R+T_I+T_F]$: Thus, from the point of view of dynamics, the model retains ambiguity. During this period of time the bone model exhibits transient behavior. Moreover, it is not clear what $\overline{N_R}$ and $\overline{N_F}$ should be for the initial period. For large times the differential equations make sense with time averages of N_R and N_F, i.e., $\overline{N_R} = N_R/T_R$ and $\overline{N_F} = N_F/T_F$. The ambiguity for all times disappears, of course, if prehistory data is an equilibrium solution.

To simplify the notation, let

$$I(a,b) \equiv \int_a^b f_a(p(s), D(s))\, ds.$$

It seems natural to define N_R as:

$$N_R(p,D,t) = \begin{cases} I[0,t], & \text{if } t < T_R; \\ I[t-T_R,t], & \text{otherwise,} \end{cases} \tag{8}$$

For N_F it is less clear. A simple choice (which we believe was used in obtaining numerical results in HMRR) is to set it to zero until $t > T_R + T_I + T_F$ (until the end of the "first" refilling period). Hence

$$N_F(p,D,t) = \begin{cases} 0 & \text{if } t < T_R+T_I+T_F; \\ I[t-(T_R+T_I+T_F), t-(T_R+T_I)] & \text{otherwise,} \end{cases} \tag{9}$$

and we define the time averages as

$$\overline{N_R}(p,D,t) = \begin{cases} \frac{I[0,t]}{t}, & \text{if } t < T_R; \\ \frac{I[t-T_R,t]}{T_R}, & \text{otherwise,} \end{cases} \tag{10}$$

and

$$\overline{N_F}(p,D,t) = \begin{cases} 0 & \text{if } t < T_R+T_I+T_F; \\ \frac{I[t-(T_R+T_I+T_F),\, t-(T_R+T_I)]}{T_F} & \text{otherwise.} \end{cases} \tag{11}$$

2.3 Parameters: defined, given and derived

A number of parameters are derived and others given by observations or constraints. Table 1 summarizes all of these and indicates whether they are defined, given, or derived. The distinction between defined, given and derived parameters is important: Owing to the large discrepancy in the size of the parameters, disregard for how these parameters are used can lead to serious loss-of-precision errors, even on double precision machines. In what follows we use the HMRR paper as a guide with regard to parameters that are 'given' (*e.g.*, experimental/observational in origin), and derived and defined, which are either created or a consequence of constraints.

The mechanical stimulus Φ_0 is a given parameter. Its value is what is required to maintain cortical bone mass in equilibrium and has been assumed to correspond to an average person who experiences about $R_L = 3000$ cpd of lower extremity loading. The initial damage D_0 is taken to be the average crack density for a 40 year old man and thus taken to be given and exact here. In HMRR this value was obtained from measurements. On the other hand, p_0 is a derived parameter. It is obtained by solving for the root p_0 of the following equation:

$$\Phi(p_0) \; = \Phi_0 = 3000 \left(\frac{891.6}{100 E(p_0)} \right)^q. \tag{12}$$

The value of q will have a bearing on the value of p_o. Nevertheless, in HMRR, they used the same p_0 regardless of the value of q — see Figure 7 of HMRR. In summary, the initial value of D is given: $D(t=0) = D_0$; the initial value of p is computed: $p(t=0) = p_0$; the values of Φ_0 and f_{a0} are given.

We define the Damage Rate Coefficient K_D as follows. The value of the mechanical stimulus Φ_0 maintains a cortical bone mass in equilibrium and is consistent with a value of 891.6 N for the load, and $q = 4$, $p = p_0$ in (12). Thus at equilibrium $\dot{D} = 0$ in (7). Hence,

$$K_D \; = \; \frac{F_s, D_0 \, S(p_0) f_{a0} \, A}{\Phi_0}, \tag{13}$$

where, in accordance to (5), we include the factor $S(p_0)$ in this calculation.[1]

3 Analysis of the BMU-MD Model

For a given load L, the steady states are found by setting the time derivatives of p and D to zero in the evolution equations. These steady state solutions, in fact, turn out to describe the stable asymptotic behavior of the model: as we will show later on, the damage equation, as originally conceived by HMRR, produces only bounded solutions; the population dynamics equation for the BMU's is bounded, by construction.

We obtain the steady states by setting the time derivatives in (6) and (7) to zero. By construction, (6) enforces the constraint $0 \leq p \leq 1$. We require that $D \geq 0$. For t sufficiently large, we set $p(t) = \hat{p}$ and $D(t) = \hat{D}$, both constant. With these, equation (6) is trivially satisfied, since

$$Q_R \, N_R(\hat{p}, \hat{D}, t) \; = \; Q_F \, N_F(\hat{p}, \hat{D}, t).$$

Furthermore, $\Phi(\hat{p}, \hat{D}, t) = \hat{\Phi}$, $A(\hat{p}) = \hat{A}$, $E(p) = \hat{E}$ are all constant. Since $\hat{D}$ is constant then its time derivative is zero. The steady values of $(\hat{p}, \hat{D})$ are obtained by solving

$$K_D \Phi(\hat{p}, \hat{D}) - F_s A \hat{D} f_a(\hat{p}, \hat{D}) = 0. \tag{14}$$

Thus values of $\hat{p}$ and $\hat{D}$ that satisfy (14) represent the fixed points of (6) and (7).

Steady states, and the effect of K_D:

[1] HMRR did not include the factor $S(p_0)$, and hence used $k_D = K_D / S(p_0)$ as their damage rate coefficient. To make the difference plain, $K_D \approx 5.57 \times 10^4$ mm/mm^2, $k_D \approx 1.85 \times 10^5$ mm/mm^2. We use K_D unless otherwise noted.

For a load $L = 891.6$ N Figure 2(a) shows the fixed point curves and how these are modified when either we use the correct value K_D or the value employed by HMRR, k_D. Clearly, there are significant differences in the outcome of numerical simulations, particularly for high porosity. Figure 2(b) and (c) show the fixed point curves for the under-stressed and over-stresssed cases, respectively. The damage apparently plays a very limited role in the under-stressed case, for low porosity. For larger values of the porosity there is a

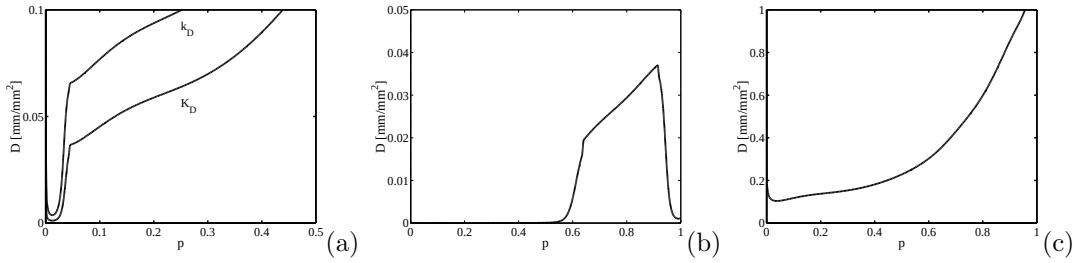

Figure 2: Fixed or stationary points of the model are depicted here as a line in the (p, D) plane. (a) For $L = 891.6\,N$, we compare the predictions using K_D and k_D. (b) Under-Stressed $L = 255\,N$ (c) over-stresssed $L = 1665\,N$. In (b) and (c) we use K_D.

significant jump in the porosity, D reaches unphysical values in this case. However, a decrease in the damage for the largest p is notably odd and can be entirely attributed to the downstream effects of Φ for large p, which in turn is being affected by the increasing value of E for the largest values of p. The over-stresssed case is characterized by commensurate effects on p and D. However, there is a sensible and dynamic interplay between porosity and damage for low values of both.

Bounded solutions for the over-stresssed case:

Since $E(p) > 0$, as prescribed by HMRR, $f_a(D, p) > 0$ except when $p = 0$ –due to $S(p)$– and $\Phi(p)$ is bounded and positive, we may thus write (7) as

$$\frac{dD}{dt} \leq g_1 \, - \, g_2 \, D,$$

where g_1, g_2 are positive and do not depend on D, which implies

$$D(t) \, \leq \, C_1(g_1, g_2), \tag{15}$$

where C_1 is a positive constant that depends on the parameters that constitute the g's. Hence, the model does not produce solutions with super linear growth, as those found numerically by HMRR. A caveat must be added, however: if the activation frequency were to become 0 then $g_2 = 0$ and blowup would be possible, but this outcome is outside of the realm of physical possibility.

The nature of oscillations in the model:

It is not unreasonable to expect oscillations in the model solution: It is composed of integro-differential equations, which can be recast as delay equations, which can potentially have oscillating solutions. Figures 4, 5 and 8 of HMRR show oscillating solutions. Are the oscillations related to the activation frequency, as claimed by HMRR? Are the oscillations, seen in the numerical results of HMRR, numerical artifices due to either p drifting outside of its range, or D becoming negative? Can the model indeed have sustained oscillations for a solution?

We perturb the steady solutions $(p(t), D(t)) = (\hat{p}, \hat{D}) + (\delta p, \delta D)$ and substitute these into (6) and (7). We get $\frac{d\delta p}{dt} = 0$. The damage equation leads to

$$\frac{d\delta D}{dt} = -\kappa_1 \delta p - \kappa_2 \delta D,$$

where the real part of $\kappa_i \geq 0$, $i = 1, 2$, and are never strictly imaginary. Therefore, if oscillations appear, they would decay exponentially; sustained oscillations are not possible. If p and D admit oscillations it is easy to see that the activation frequency will also have oscillations. However, since only decaying oscillations are admissible it is not possible (for a fixed set of parameters) to have sustained oscillations due to the activation frequency.

4 The BMU-MD Model, Revisited

In the previous section we focused on characterizing certain aspects of the model, as it was formulated in HMRR. Among other things we found that the model has bounded damage for any level of applied stress, that the model solutions are very sensitive to some of the parameterizations, and that the behavior of the model when p approaches 1 is unphysical. Here we consider how the BMU-MD model dynamics are modified by replacing the damage growth term in the damage equation.

4.1 A Relative Damage Rate Equation

The original HRMM model was shown to yield, for p sufficiently far from 1, comparatively reasonable results when the bone is under-stressed. However, there is bounded growth of the damage, irrespective of the load, for non-vanishing values of the activation frequency. The expectation, however, is that over-stresssed conditions should yield a phenomenology consistent with the experiments reported by Cotton, Pattin and others [9, 8, 10].

In [10] (see also [9]) they perform an empirical fit of the creep strain of cortical bone subjected to strains. The bone specimens come from cadavers and are thus not subject to damage repair. The data shows that the cyclic strain in the bone, over some threshold, leads to progressive damage. It may eventually lead to catastrophic levels, provided the load is sufficiently high and/or the sample is subjected to stresses for long enough periods of time. Furthermore, the data shows that the history of bone degradation depends on whether the stresses are compressive or tensile.

The damage rate equation, as given by (7), is only partially relative to the damage via the second term on the right hand side. Moreover, as demonstrated in the previous section, even when the bone is over-stresssed it is not possible to obtain unmitigated growth in time for the damage. In particular, the modelling philosophy of HMRR for the damage accumulation term, *i.e.*, the term $K_D\Phi$, is consistent with this form for the creep strain. Obviously, in this case $D \leq g_1 t$, where $g_1 > 0$ is an upperbound to $K_D\Phi$; Φ, as we know, is bounded. The damage thus grows at most linearly.

If we resort to the fundamentals of fracture mechanics for the bone damage development, an alternative model for the permanent strain, reminiscent of Paris Law (see [11]), relates the crack growth rate under a fatigue stress regime to the stress intensity factor as a power law – below the threshold crack size, the crack will not grow. This leads to a damage accumulation, in terms of a function F, of the form

$$D \propto= \frac{1}{F((t_f - t))}, \tag{16}$$

for $D > D_{th}$, some threshold damage, and $D = D_{th}$ otherwise. This form presumes no damage repair. Here, t_f would depend on L and E, perhaps as suggested by (1). We will show that (16) would be qualitatively similar to the data presented in [8] in their Figure 3, *i.e.*, a period of accumulating damage followed by catastrophic failure, given repeated loading above some threshold, and can be made to fit the data studied by Pattin and Collaborators [10], thus offering an alternative and perhaps simpler description of the damage accumulation term. We propose a power-law dependence for the relative damage $\overline{D} \equiv D/D_0$ as an alternative to the logarithmic fit suggested in [10]. A secondary aim is to show that replacing the damage growth term in (7) by a Paris-law leads to significant increases in the resulting damage when the bone is over-stresssed. We expect, however, that in the under-stressed case, the behavior of the model to be not significantly different from the model in its original inception, for short times.

The proposed alternative damage equation is

$$\frac{d\overline{D}}{dt} = c_m \left(\frac{L}{E(p)}\right)^q \overline{D}^m \overline{D} \; - \; F_s A \, \overline{D} f_a(p, D), \tag{17}$$

for $D \geq D_{th}$, where $c_m \geq 0$, and $m \geq 1$. HMRR suggest that there should be an equilibrium damage state, in which case c_m is tuned to obtain $d\overline{D}/dt = 0$, say, for the conditions of load $L = 891.6$ N, $E(p_0)$, f_{a0}, and $D = D_0$. The exponent m is a new parameter in the problem whose numerical value in the example calculations will be taken to be 1; the reason for this choice of m will become apparent in what follows.

A threshold for the relative damage to grow exponentially and irretrievably is given by

$$\overline{D} > \left(\frac{F_s A f_a E^q}{c_m L^q}\right)^{1/m}.$$

This is the case when the damage accumulation is more prominent than the damage repair term. From this expression we see that increasing the load L lowers the threshold. Moreover, the larger the load, or the exponent m, the sooner the instability occurs. Blowup leads to full decoupling of the activation frequency on the damage, *i.e.*, $f_{a(damage)} = f_{a(max)}$ and thus no feedback is possible in the porosity, other than a readjustment in the porosity. We thus expect the coupled model to exhibit irretrievable growth in the damage with no change on the porosity, beyond an adjustment in its value shortly after the blowup. Whether this is the correct behavior of under-stressed bone is beyond the scope of this work.

Figure 3 shows the critical points in the (p, D) plane for $m = 1$. The case corresponding to $L = 891.6$

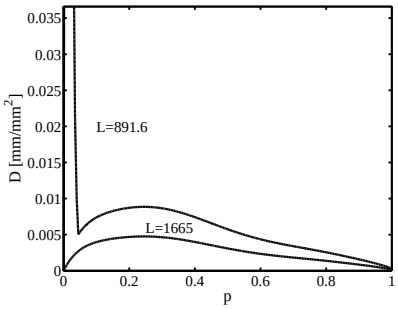

Figure 3: Porosity and damage fixed points, using (17) with $m = 1$ for the damage equation. Computed using $L = 891.6$ N, and the over-stresssed case with $L = 1665$ N.

N is a tuned threshold for the model (the c_m is set with this load). Interestingly, steady solutions exist for porosities higher than about 0.0442, which is the value of p_0. For loads higher than $L = 891.6$, steady solutions are defined for all values of p and D. These higher load cases generate curves that would be located below the $L = 891.6$ curve. The quick decrease in the damage for high porosity in the over-stresssed case (where we take $L = 1665$), is related to the anomalous increase in E for high values of p (see Figure 1a, also comments in the following subsection).

Figure 4 show the porosity, damage, and activation frequency as a function of time with the new dynamics. In the under-stressed cases, the second term in the damage equation dominates. Figure 4a shows several cases with low loads. These figures show qualitative similarity with the under-stressed case of the original model (shown in Figure 5, which appears in Appendix C).

Figure 4b shows the over-stresssed case, as a function of the load L. As expected in over-stresssed conditions, provided enough time passes, the damage can grow exceedingly large, leading to bone failure.

García-Aznar *et al* [3] adopted a form for the damage accumulation term, consistent with the fit suggested in [10]. Moreover, they defined two different damage formation modes, one for tension and one for compression. The rate in both cases is essentially exponential in the damage itself. Our goal here is to suggest that the power law and the exponential form for the damage accumulation term in the damage rate equation are

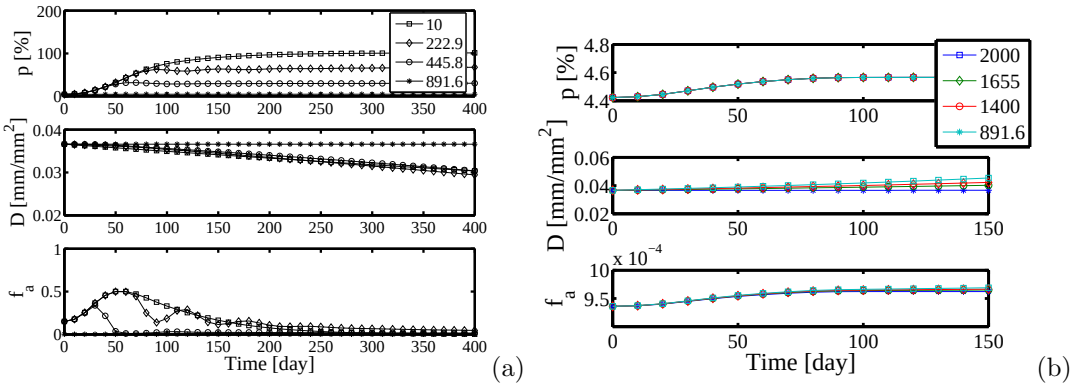

Figure 4: Porosity, damage, and activation frequency as a function of time, using (17) with $m = 1$. (a) Under-stressed. (b) Over-stressed.

equivalent. To this end, we ignore the damage repair term in the damage rate equation. Furthermore, we will opt for using their definition of the damage: Let $\mathcal{D} := 1 - E/E_0$, where E_0 corresponds to a reference value of the elastic modulus of the undamaged bone. In García-Aznar this damage is described by

$$\mathcal{D} \propto b_1 - b_2[\ln(b_3 - c_g\, t/t_f)]^n, \tag{18}$$

where b_1, b_2, and c_f are constants tuned to agree with results in [10]. Moreover, under tensile stress $n = 1/2$, $b_1 = 1$, $b_2 > 0$, $0 < b_3 < 1$; under compression, $n = 1$, $b_1 = 0$, $b_2 > 0$, $b_3 = 1$. In contrast, in terms of the power law damage equation prediction for $\overline{D}$, ignoring damage repair, and with $\mathcal{D} = \overline{D} - \mathcal{D}_0$, is of the form

$$\mathcal{D} \propto \frac{b_4}{(1 - c_f\, t/t_f)^{1/m}} - \mathcal{D}_0, \tag{19}$$

where b_4 can be written in terms of m, t_f, and c_f.

Both forms can be made to pass through $\mathcal{D} = 0$ at $t = 0$ with proper tuning of the parameters. Both exhibit divergent behavior, at $t_f b_3/c_g$ and t_f/c_f, respectively. The values of the parameters in the exponential damage accumulation term appear in [3], in both the compressive and the tensile cases. They are chosen to match the fit suggested by [10]. Assuming that (18) is exact in its representation of the damage accumulation due to stresses one can write a series about $t = 0$ of (18) and (19) and term by term comparison shows that for both tensile and compressive forces $m = 1$, and that $\mathcal{D}_0 = b_4$ is the compressive case and $\mathcal{D}_0 \neq b_4$ for the tensile case and both of these parameters can be fixed uniquely for a reasonable fit. This implies that both the exponential and the power law fits are equally capable of fitting the experimental data. (Of some mathematical interest, writing a series expansion near the singular point, a Laurent expansion for the powers of the logarithm function, shows that the leading order behavior requires a complex representation. This is obviously not the case for the power law representation).

Formally, the power law is appealing in its simplicity and its generality. It leads to a bone damage rate equation that is considerably simpler to analyze mathematically. Moreover, since it is inspired by a Paris-law for damage of materials, it is presumably possible then to relate certain bone material properties to an extensive materials literature related to fatigue of materials under repetitive use.

5 Conclusions

Restating the BMU-MD model proposed by HMRR in a balanced and concise way lead to a set of equations amenable to simple mathematical analysis. We made the simplifications considering that a practical model would also be stable numerically; given the extreme spatio-temporal scales of its parameters, the numerical simulations of the equations were vulnerable to serious numerical loss-of-precision errors.

Analysis of the steady states of the model yielded global behavior of the solutions, given a load L; ambiguity for times shorter than the full remodeling cycle means that the model has to run from an equilibrium point for a full cycle before making changes in its parameters. Once the bone parameters are determined the only remaining dynamic parameter is the load. Furthermore, knowing the global solutions it was also possible to suggest phenomenological simplifications of the model that lead to the same qualitative behavior. The empirical fit of HMRR of the Young's modulus was found to be problematic for large values of porosity: the Young's modulus was found to be finite and nonzero for porosity equal to 1, and further, to be an increasing function in the neighborhood of high porosity. This has a bearing on the activation frequency as well as on the damage-forming term in the damage equation in the original model. When we replaced the Young's modulus with a monotonically decreasing function we found that the "mechanical stimulus" Φ has extremely limited dynamics, leading to problems in the damage equation, as originally conceived. This problem is obviated in the power-law alternative formulation of the damage-causing term as it does not depend on the mechanical stimulus. Furthermore, our analysis presents arguments for considerably simplifying the material properties, as well as parts of the activation frequency function. The term associated with disuse in the activation frequency was also shown to be well approximated by a considerably simpler expression, without loss of quantitative and qualitative fidelity.

The damage equation, in the HMRR formulation, was found to have bounded solutions for finite values of the parameters, regardless of the level of the stress on the bone. A power-law alternative of the model was suggested here as a dynamic for the damage. This model is inspired by the bone data analyzed in [8] from experiments that show creep strain behavior and possible failure under loading. We also found that making the damage rate relative to the damage itself leads to significant changes in the damage in the over-stresssed case. Moreover our calculations show that in the original model the dependence of the porosity on the damage might be too weak, particularly in the over-stresssed case, where it is possible to get unrealistic values in the damage with little change in the porosity. Excluding exponential growth or decay a balance in the damage equation is obviously possible. Since the coupling between porosity and damage is weak the stability of the system is nearly entirely controlled by the damage equation and is thus most always a trivially unstable fixed point.

Restating the BMU-MD model allows one to compare with the recent model of García-Aznar *et al* [3]. This latter phenomenological model is capable of modeling stress fractures, among other things, and it has been shown to have significant predictive potential. When the model by García-Aznar *et al.* is stripped of some phenomenological complexities it becomes clear that it shares some common characteristics with the BMU-MD model: this is because it uses a population dynamics equation for the BMU's and an equation for the damage rate that involves a formation and a repair term. We opted for a power-law damage production term and García-Aznar *et al* for an exponential damage production term. We show that either of these will give qualitatively good fits of the damage data from experiments and that both models will exhibit similar behavior. In view of this the model of García-Aznar *et al* is shown to have important similarities to the HMRR model. There are important distinctions between the models as well: We show in this study that the HMRR specification of the bone properties in terms of porosity alone leads to weak coupling in the steady solutions of the porosity and the damage under fixed loads. The material properties of the bone, *i.e.* the effective surface area and the Young's modulus, are entirely fitted to data in terms of porosity in the HMRR specification of the BMU-MD model, whereas it is specified in terms of the damage and porosity in the García-Aznar *et al.* model. In [3] the authors opted for a different model for the Young's modulus by taking into account the loss of stiffness due to damage and with this change they obtained a richer phenomenology, it strongly suggests that the improvements in the HMRR formulation of the BMU-MD model will be obtained by focusing on the specification of the material properties of the bone.

Acknowledgments

The authors are grateful to Scott Hazelwood for several useful correspondences. This work was performed in part while JMR was a PIMS faculty visitor at Simon Fraser University and a visitor at Los Alamos National Laboratory. JMR was supported by NSF Grant DMS-327617 and DOE Grant DE-FG02-02ER25533. RC was supported by an NSERC Canada Discovery Grant. YJ was supported by the US Department of Energy under Contract No. DE-AC52-06NA25396.

References

[1] S. J. Hazelwood, R. B. Martin, M. M. Rashid, and J. J. Rodrigo, "A mechanistic model for internal bone remodeling exhibits different dynamic responses in disuse and overload," *Journal of Biomechanics*, vol. 34, pp. 299–308, 2001.

[2] M. Doblaré, J. García, and M. Gomez, "Modelling bone tissue fracture and healing: a review," *Engineering Fracture Mechanics*, vol. 71, pp. 1809–1840, 2004.

[3] J. M. García-Aznar, T. Rueberg, and M. Doblaré, "A bone remodelling model coupling microdamage growth and repairing by 3d bmu-activity," *Biomechanics and Modeling in Mechanobiology*, vol. 4, pp. 147–167, 2005.

[4] C. J. Hernandez, G. S. Beaupré, and D. R. Carter, "A model of mechanobiologic and metabolic influences on bone adaptation," *Journal of Rehabilitation Research and Development*, vol. 37, pp. 235–244, 2000.

[5] C. J. Hernandez, G. S. Beaupré, T. S. Keller, and D. R. Carter, "The influence of bone volume fraction and ash fraction on bone strength and modulus," *Bone*, vol. 29, pp. 74–78, 2001.

[6] J. S. Nyman, S. J. Hazelwood, J. J. Rodrigo, R. B. Martin, and O. C. Yeh, "Long stemmed total knee arthroplasty with interlocking screws: a computational bone adaption study," *Journal of Orthopaedic Research*, vol. 22, pp. 51–57, 2004.

[7] J. S. Nyman, O. C. Yeh, S. J. Hazelwood, and R. B. Martin, "A theoretical analysis of long-term biphosphonate effects on trabecular bone volume and microdamage," *Bone*, vol. 35, pp. 296–305, 2004.

[8] J. R. Cotton, P. Zioupos, K. Winwood, and M. Taylor, "Analysis of creep strain during tensile fatigue of cortical bone," *Journal of Biomechanics*, vol. 36, pp. 943–949, 2003.

[9] W. Caler and D. R. Carter, "Bone creep fatigue damage accumulation," *Journal of Biomechanics*, vol. 22, pp. 625–635, 1989.

[10] C. A. Pattin, W. E. Caler, and D. R. Carter, "Cyclic mechanical property degradation during fatigue loading of cortical bone," *Journal of Biomechanics*, vol. 29, pp. 69–79, 1996.

[11] S. Suresh, *Fatigue of Materials*. Cambridge, UK: Cambridge University Press, 1991.

[12] R. B. Martin, "A theory of fatigue damage and repair in cortical bone," *Journal of Orthopaedic Research*, vol. 10, pp. 818–825, 1992.

[13] R. B. Martin, N. A. Sharkey, and D. B. Burr, *Skeletal Tissue Mechanics*. New York: Springer Verlag, 1998.

[14] R. B. Martin, "Porosity and specific surface of bone," *Critical Reviews in Biomedical Engineering*, vol. 10, pp. 179–222, 1984.

[15] A. Iserles, *A First Course in Numerical Analysis of Differential Equations.* Cambridge: Cambridge University Press, 1996.

[16] X. Wang and Q. Ni, "Determination of cortical bone porosity and pore size distribution using a low field pulsed nmr approach," *Journal of Orthopaedic Research*, vol. 21, pp. 312–319, 2003.

Model Parameters

Table 1 lists all of the parameters used in the model.

Table 1: *Model constants and other parameters defined, given, or derived.*

symbol	value	units	definition
c_1	-	1	$e^{-k_b k_c}$
c_2	-	days^{-1}	k_b
c_3	-	1	$\frac{f_{a(max)}-f_{a0}}{f_{a0}} e^{-k_r f_{a(max)}}$
c_4	-	mm	$\frac{k_r}{D_0} f_{a(max)}$
c_5	-	mm/mm^2	k_D
c_p	1.90		see (17)
K_D	-	mm/mm^2	$S(p_0)k_D$
k_D	-	mm/mm^2	see (13)
A_0	2.84×10^{-2}	mm^2	-
$f_{a(max)}$	0.5	mm^{-2} days^{-1}	-
m	-	1	see (17)
T_R	24	days	-
T_I	8	days	-
T_F	64	days	-
R_L	3000	days^{-1}	-
k_b	6.5×10^{10}	days-1	-
k_c	9.4×10^{-11}	days	-
k_r	-1.6	mm^2 days	-
p_0	-	1	see (12)
D_0	0.0366	mm/mm^2	-
Φ_0	1.875×10^{-10}	days-1	-
f_{a0}	0.0067	# BMU's/mm^2/day	-
F_s	5	mm^{-2}	see (13)

Numerical Methodology

The extreme disparity in size of variables and parameters in the model can easily lead to numerical loss-of-precision errors. The integro-differential equations were solved using a variable order stiff solver of type 'backward difference formula' (see [15]). The tolerances were set to machine epsilon. The solver was used inside an adaptive trapezoidal quadrature for the integrals.

The code properly converged when the adaptive trapezoidal integrator was set to fixed time steps. The test was made as follows: we replaced the integrand with a function which we could integrate analytically. The code was kept intact otherwise. We then compared the relative error with the expectation that the quadrature scheme should converge at a rate of Δt^2, where Δt is the time step. We found that e.g., for

$\Delta t = 1.0$, the relative error is $10^{-3.0793}$; for $\Delta t = 0.25$, the relative error is $10^{-4.2833}$; for $\Delta t = 0.0625$, the relative error is $10^{-7.4874}$. A polynomial fit of the logarithm of the relative error in terms of the logarithm of the time step yielded a slope of 2, thus confirming that we have convergence at the correct rate. Separately we tested the BDF portion which advances the differential equation. The scheme was adaptive so we confirmed that the tolerances were met *post-facto* and that the error was well below the trapezoidal integrator. Hence, the local error was controlled by the trapezoidal quadrature and thus the overall solution was order 2 with respect to fixed time step.

Numerical Results and Comparison with HMRR

In this section we present our numerical findings and compare them with those of HMRR on their BMU-MD model. We have shown that our results are consistent with the analysis and that we use convergent codes. Since the numerical simulations were instrumental in the HMRR paper to explain or illustrate the model's characteristics (and thus also critical in setting forth a path of improvement in the modeling effort) it is useful to highlight the differences in the results. Here we are simulating the model as derived by HMRR, without changes to the damage equation or the material properties of the bone. We emphasize here that differences are not due to the adoption of a different model, but rather, due to our implementation of a stable numerical algorithm and the careful calculation of wide ranging parameters. As we will see, our numerical results are consistent with the analytical estimates presented in this study. In what follows we will use the value of the proportionality constant in (8) which includes the factor of $S(p_0)$, *i.e.* K_D, rather than k_d.

(i) **Effect of Under-Stressing**

In the case of under-stressing, Figure 5 shows qualitative agreement with HMRR. (We show only time 600 days in order to show more clearly the initial stages of the evolution. Plotting to 2000 days shows nothing that cannot be inferred in the truncated solutions.). Quantitative differences are primarily due to the use of K_D versus k_D. We find that the ringing in the HMRR results is spurious numerical artifacts. Contrary to HMRR, the damage plot in Figure 5 does not show any unbounded growth.

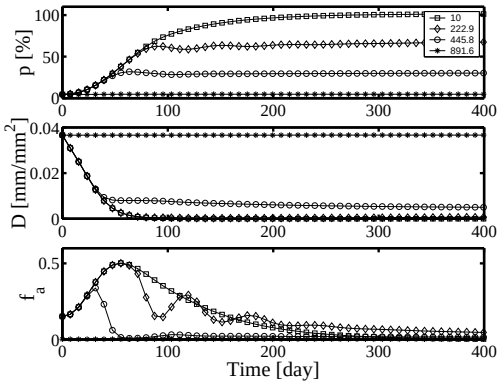

Figure 5: Porosity, damage, and activation frequency for the under-stressed case, as a function of the load L. This corresponds to Figure 4 of HMRR.

As we mentioned in the Section 3 it is not possible to obtain sustained oscillations in the dynamic variables p and D. Oscillations, however, are not ruled out, and in fact are usually expected in delay equations. The ringing that appears in the HMRR results for dynamic variables in the transient period, however, are mostly a numerical artifact. Longer-period oscillations in the HMRR results related with the dynamic variables, *not* associated with changing the parameters T_I, T_R, and T_F, were most likely induced by allowing p and D to go out of range (inducing complex eigenvalues in the linearized equations).

(ii) **Effect of Changing** $f_{a(max)}$

For the activation frequency the situation is portrayed in Figure 5, for $L = 222.9N$ as an example. The main difference between our results and HMRR is quantitative: in HMRR the oscillations are more pronounced. We found that for loads in the 240-400 N range, approximately, there is a significant increase in decaying oscillations in f_a. In fact the oscillations disappear well outside of this load range.

The primary effect of changing $f_{a(max)}$ is to modify the fixed point curves. Figure 6 shows the long-time solutions for a variety of $f_{a(max)}$ and under the action of two different loads. Changing $f_{a(max)}$ has little

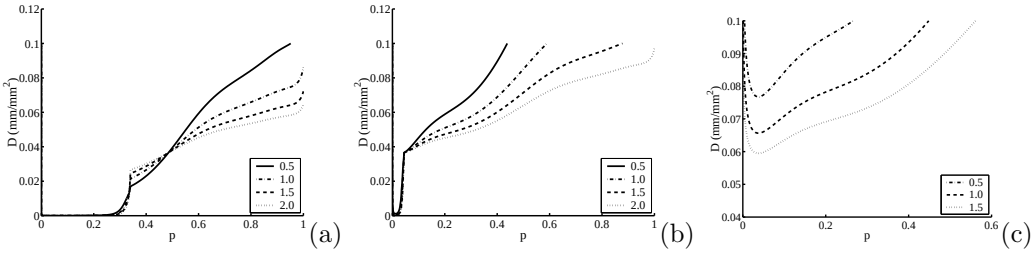

Figure 6: The effect of increasing $f_{a(max)}$ on the fixed point curves. (a) $L = 445N$, (b) $L = 891.6N$. (c) $L = 1655N$. Note, the case $L = 1655$ and $f_{a(max)} = 0.5$ is illustrated in Figure 2(b) and is outside of the plot range chosen to make these figures.

effect for small p and D, however, for p sufficiently large, increasing $f_{a(max)}$ decreases the damage. This is all in contrast to the HMRR results wherein increases in oscillations were ascribed to changes in $f_{a(max)}$.

Lastly, we notes that a change that does lead to decaying oscillations is changes in the parameters T_R, T_I, and T_F - this can be seen both numerically and via the spectrum of the linear operator associated with the delay equations. However, these parameters are set by nature.

(iii) **Effect of Over-stressing**

Figure 6 of HMRR shows that overloading ($L = 1655N$) leads to exponentially growing porosity and activation frequency. Figure 7 of HMRR shows that $q = 8$ leads to similar exponential growth in porosity and damage. In accordance with our boundedness estimate, neither the porosity nor the damage will blow up –for porosities that are reasonable, i.e. not very close to 1, where the model is flawed due to the polynomial approximation of the Young's modulus –. Figure 7 shows the results of over-stressing. We observe no super-linear growth, in agreement with the estimates in Section 3.

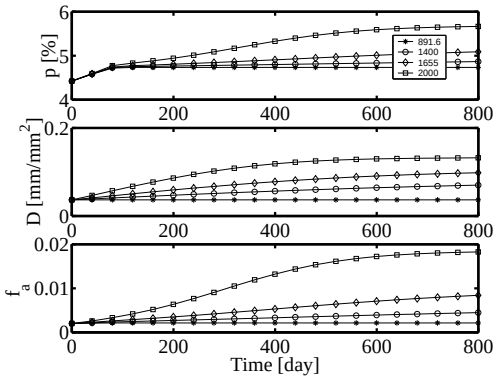

Figure 7: Porosity and activation frequency for the over-stressed case, as a function of the load L. This corresponds to Figure 6 of HMRR

(iv) **Effect of Changing** q

Finally, a few comments on varying q. Low values of q ($q = 1, 2, 3$) give negative activation frequencies and hence are not physically-meaningful; $q > 4$ also produces a negative activation frequency at large time.

Neither of these are noted in Figure 7 of the HMRR paper. Also HMRR obtained blowup for $q = 8$, which is most likely a numerical artifact.

Modeling Simplifications and Alternative Parameterization

Simplifying the Activation Frequency: One simplification is related to exploiting the limited range of porosity associated with specific bone types: for example in [16] it was reported that the porosity of Haversian canals is less than 10% for average people below 50 years of age, and at worst around 30% for females over 80 years old. As HMRR uses parameters (Φ_0 and q and f_{a0}) derived for Haversian canals or cortical bones, there must be a limited range of porosity (e.g. $p < .3$) where the model is valid. Considerable simplification is possible in the expression for the activation frequency, the result of which changes in an imperceptible manner the results from both a qualitative and quantitative point of view. For example, one can replace (5) by the expression

$$f_{a(disuse)} = \begin{cases} \frac{f_{a(max)}}{1+c_1} & \text{if } \Phi < \Phi_0; \\ 0 & \text{otherwise,} \end{cases} \tag{20}$$

This replacement can be justified as follows: the upper bound on the relative magnitude of the derivative of $f_{a(disuse)}$ with respect to Φ in the range $[0, \Phi_0]$ is no greater than 10^{-3}.

Bone Material Parameterizations: $E(p)$ and $S(p)$ have an important role to play in the damage equation. There are two issues here: (i) sensitivity in the modeling of the modulus and the specific area, (ii) $E(p)$, as prescribed by HMRR, has nonsensical characteristics for high values of p, namely the Young's modulus increases in the neighborhood of p close to 1.

The choice of a high order polynomial fit for $E(p)$ and $S(p)$ makes model simulations very sensitive to numerical error. We examined the effects of simplifying the empirical functions $E(p)$ and $S(p)$ (Figure 1a,b). The curves are not very intricate, suggesting that a lower oder polynominal fit would be suitable. It is easy to see that the relative sensitivity $|(\partial\Phi/\partial E)/\Phi|$ for the range of values of E given in Figure 1a is at most 10^{-3}. We confirmed our claim by using a second degree polynomial expressions for both (2) and (3) and found that the results changed very minimally compared to using the higher degree polynomial counterparts, especially with regard to final steady states. Here we used the higher order polynomial expressions to generate data to be interpolated. Piece-wise cubic splines do an even better job at following the higher order polynomial fit for $S(p)$ and $E(p)$ with a marginal increase in numerical sensitivity. In conclusion, a much lower polynomial fit would be adequate in interpolating the experimental data, and would be preferred from a computational point of view.

From a modeling standpoint, the more important issue is the validity of the interpolated expression for $E(p)$. In [14] data is presented over the full range of p and hence a fit for $S(p)$ (which is more sensibly fitted with lower order splines) should be adequate for modelling $S(p)$, especially for high p. The modulus $E(p)$, on the other hand, is questionably characterized in the immediate neighborhood of $p = 1$.

We can consider a constitutive relation for E as in Figure 1c, where E decrease monotomically to $p = 1$. Since the modification to our original $E(p)$ is for high values of p, the function $f_{a(disuse)}$ does not change in any way and thus the activation frequency remains the same. Therefore there is no change to the p evolution equation. The main modification will be seen in the term $K_D\Phi$ of the original damage equation (8) wherein the mechanical stimulus becomes unbounded as p approaches 1. The original BMU-MD model will thus experience catastrophic rates of damage, which may be a sensible thing to expect. Next we examine what happens to the damage equation for the middle to high range of p: if the damage equation has a Paris-law type damage-forming term the mechanical stimulus does not appear explicitly, however the ratio $L/E(p)$ appears and thus one can obtain irretrievable damage if either the bone is stressed repeatedly, provided it is done so aggressively, or the material is too sensitive to damage because its Young's modulus is too low.